**Supplementary material**

# Benzoyl Chloride Derivatization Improves Selectivity and Sensitivity of Lipidomic Quantitation in Human Serum of Pancreatic Cancer Patients Using RP-UHPLC/MS/MS

Ondřej Peterka[1], Zuzana Lásko[1], Robert Jirásko[1], Petra Peroutková[1], Anna Taylor[1], Beatrice Mohelníková-Duchoňová[2], Irena Kozubíková[2], Martin Loveček[3], Bohuslav Melichar[2], and Michal Holčapek[1,*]

[1]University of Pardubice, Faculty of Chemical Technology, Department of Analytical Chemistry, Studentská 573, 53210 Pardubice, Czech Republic

[2]Palacký University Olomouc and University Hospital, Faculty of Medicine and Dentistry, Department of Oncology, Zdravotníků 248, 775 20 Olomouc, Czech Republic

[3]Palacký University Olomouc and University Hospital, Faculty of Medicine and Dentistry, Department of Surgery, Hněvotínská 3, 779 00 Olomouc, Czech Republic

*Corresponding author: Michal Holčapek, Tel.: +420466037087; Fax: +420466037068; Email: Michal.Holcapek@upce.cz

**Table of content**

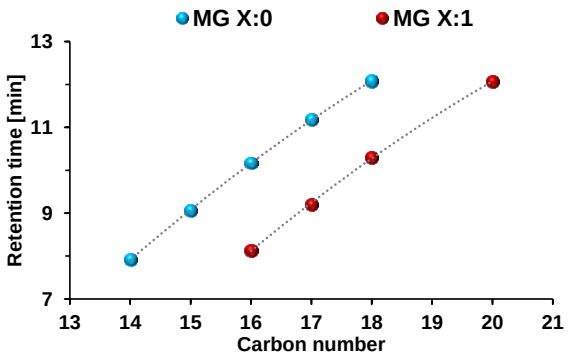
MG X:0
MG X:1
Retention time [min]
Carbon number

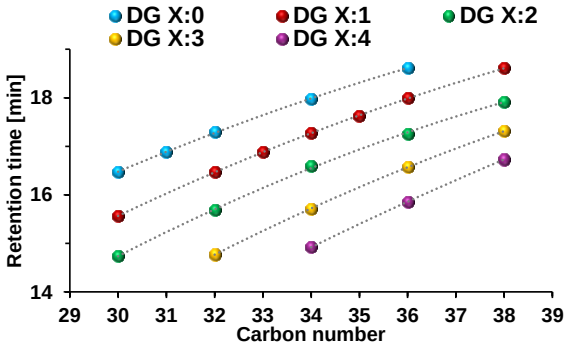
DG X:0
DG X:1
DG X:2
DG X:3
DG X:4
Retention time [min]
Carbon number

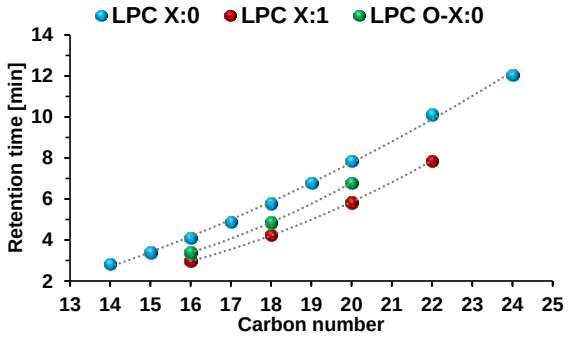
LPC X:0
LPC X:1
LPC O-X:0
Retention time [min]
Carbon number

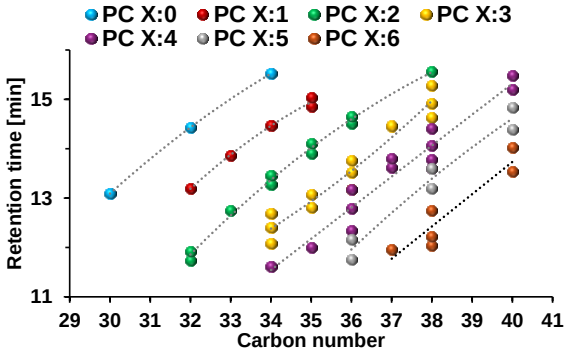
PC X:0
PC X:1
PC X:2
PC X:3
PC X:4
PC X:5
PC X:6
Retention time [min]
Carbon number

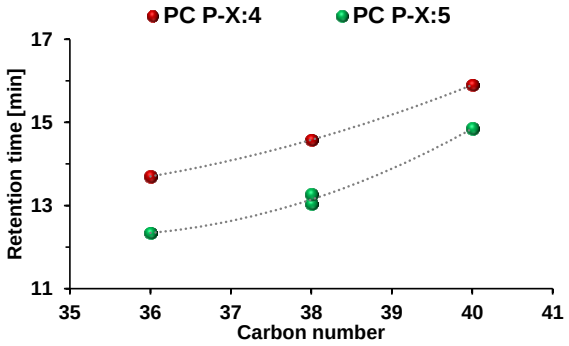
PC P-X:4
PC P-X:5
Retention time [min]
Carbon number

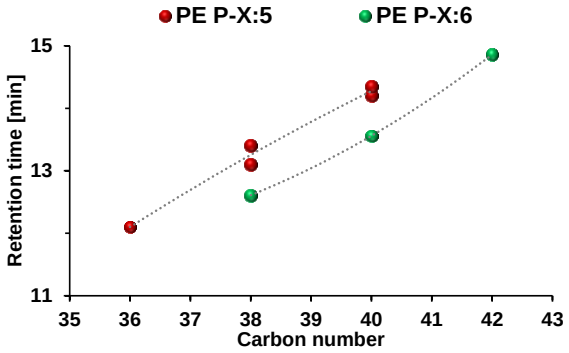
PE P-X:5
PE P-X:6
Retention time [min]
Carbon number

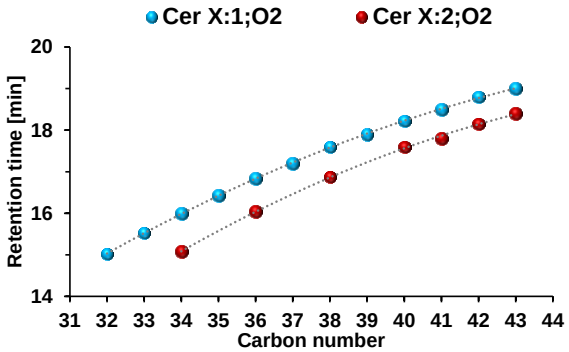
Cer X:1;O2
Cer X:2;O2
Retention time [min]
Carbon number

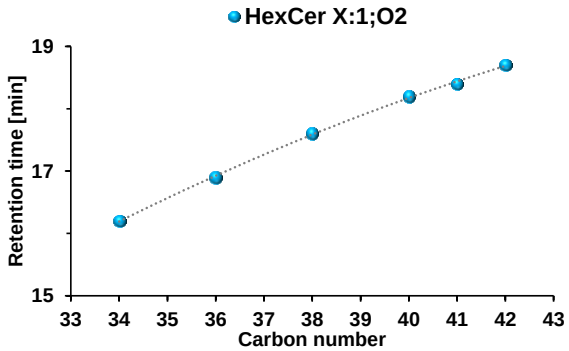
HexCer X:1;O2
Retention time [min]
Carbon number

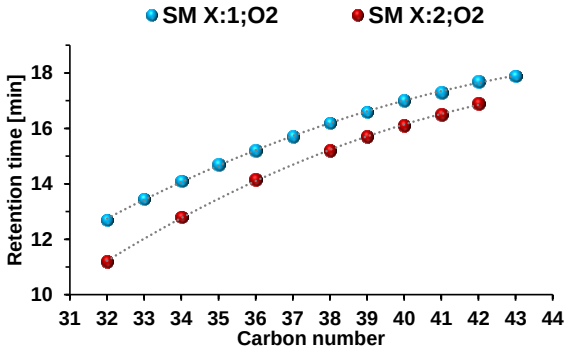
SM X:1;O2
SM X:2;O2
Retention time [min]
Carbon number

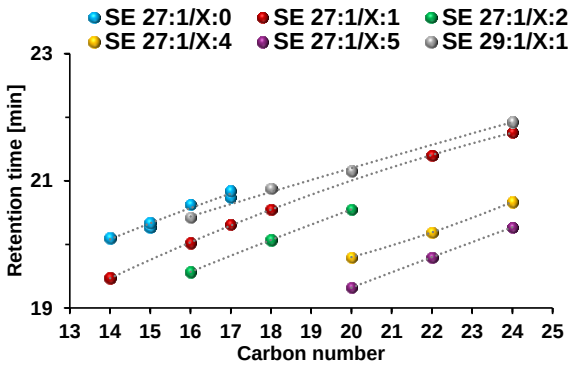
SE 27:1/X:0
SE 27:1/X:1
SE 27:1/X:2
SE 27:1/X:4
SE 27:1/X:5
SE 29:1/X:1
Retention time [min]
Carbon number

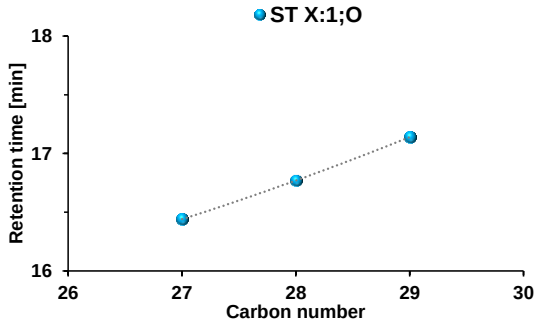


**Figure S1**: Graphical visualization of dependence of retention times on the carbon number, where X represents the carbon number. The number of double bond(s) for each lipid is written after the colon.

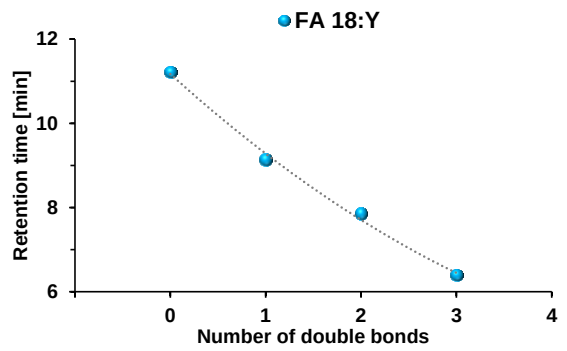
FA 18:Y
Retention time [min]
Number of double bonds

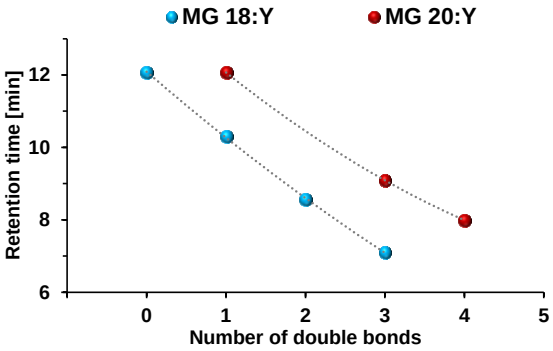
MG 18:Y
MG 20:Y
Retention time [min]
Number of double bonds

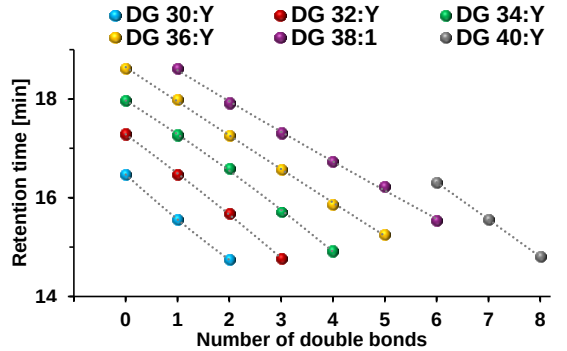
DG 30:Y
DG 32:Y
DG 34:Y
DG 36:Y
DG 38:1
DG 40:Y
Retention time [min]
Number of double bonds

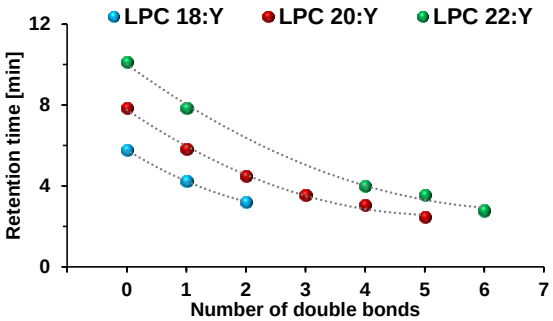
LPC 18:Y
LPC 20:Y
LPC 22:Y
Retention time [min]
Number of double bonds

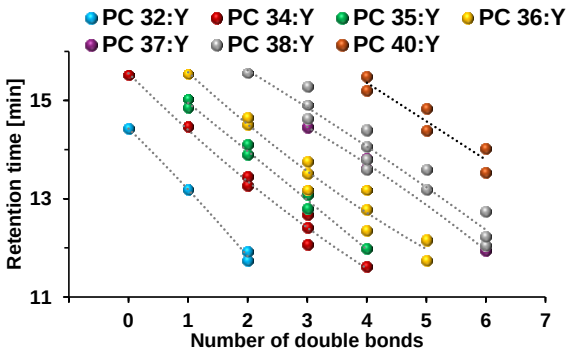
PC 32:Y
PC 34:Y
PC 35:Y
PC 36:Y
PC 37:Y
PC 38:Y
PC 40:Y
Retention time [min]
Number of double bonds

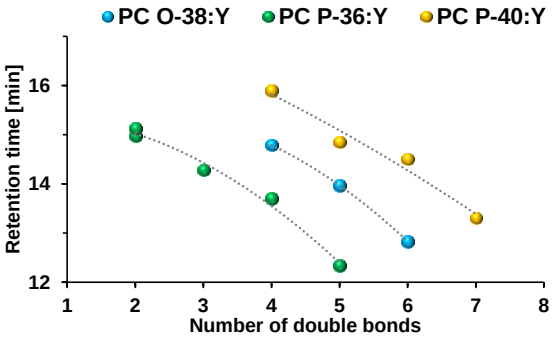
PC O-38:Y
PC P-36:Y
PC P-40:Y
Retention time [min]
Number of double bonds

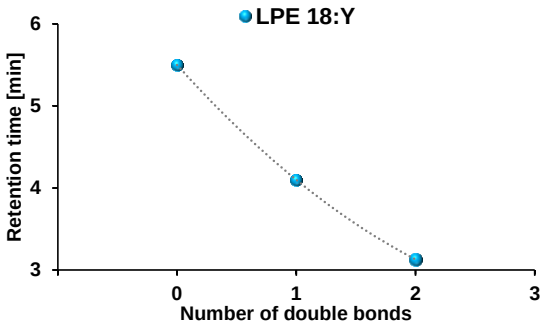
LPE 18:Y
Retention time [min]
Number of double bonds

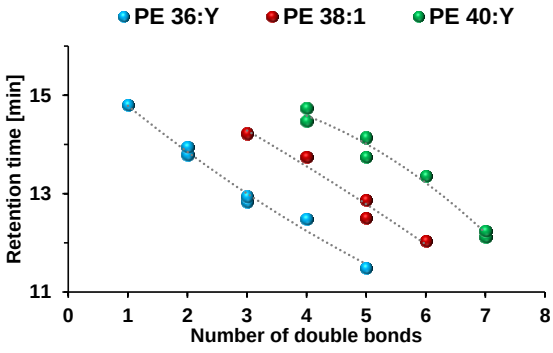
PE 36:Y
PE 38:1
PE 40:Y
Retention time [min]
Number of double bonds

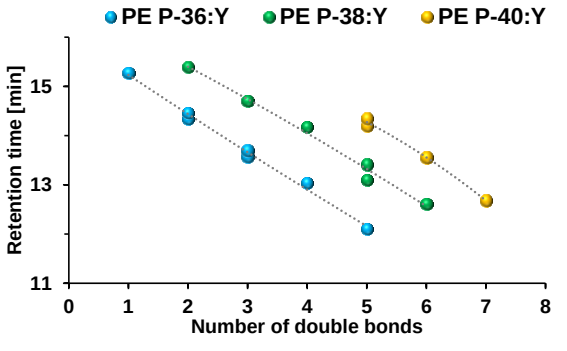
PE P-36:Y
PE P-38:Y
PE P-40:Y
Retention time [min]
Number of double bonds

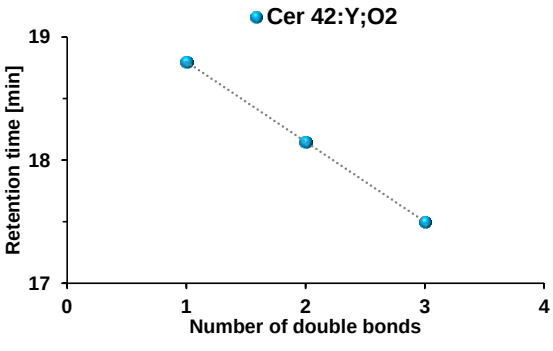
Cer 42:Y;O2
Retention time [min]
Number of double bonds

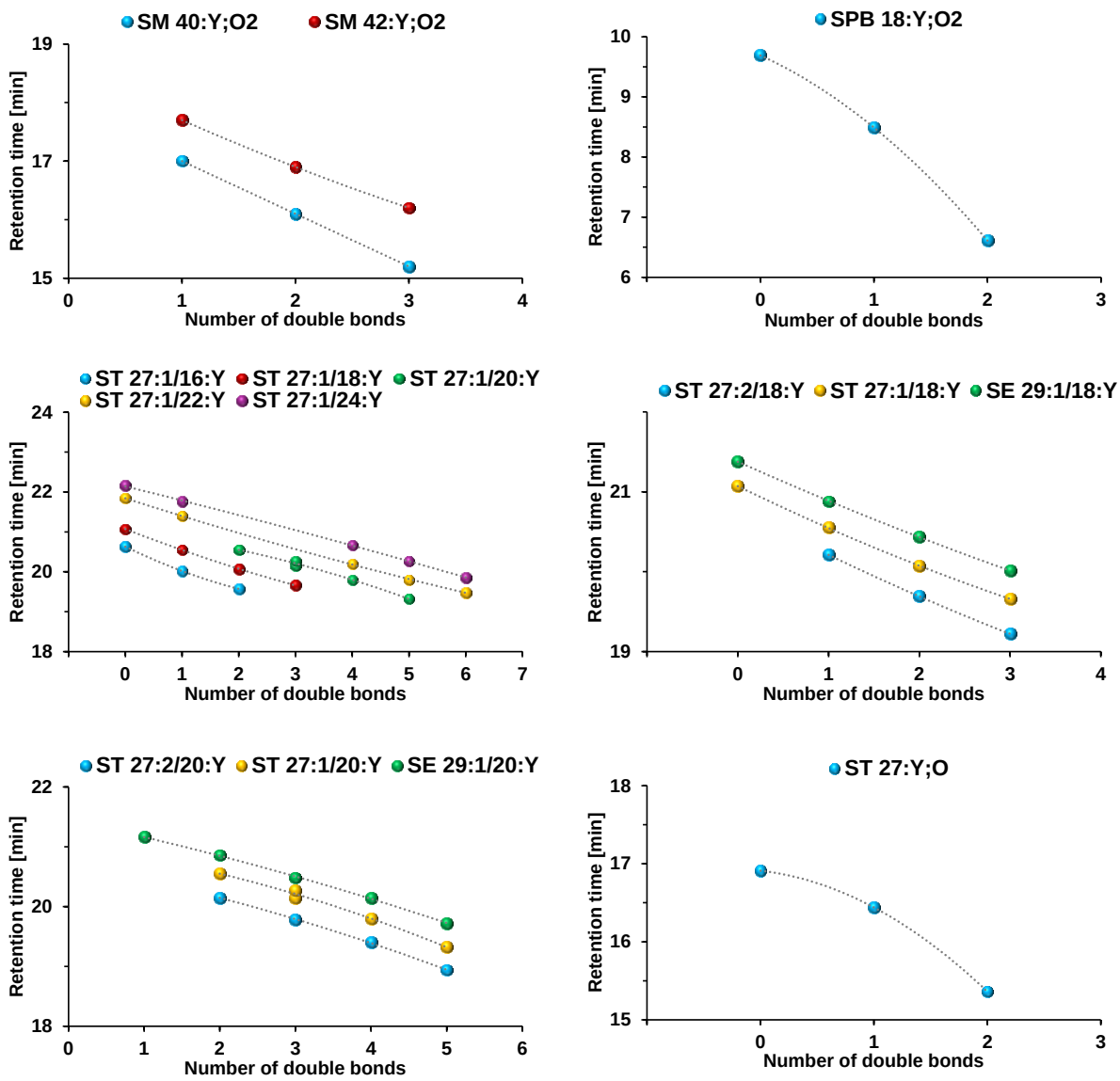


**Figure S2**: Graphical visualization of dependence of retention times on number of double bond(s), where Y represents the number of double bond(s). The total carbon number for each lipid is written before the colon.

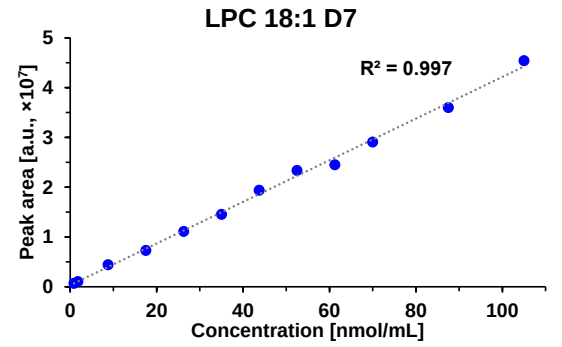
LPC 18:1 D7
R² = 0.997
Peak area [a.u., ×10⁷]
Concentration [nmol/mL]

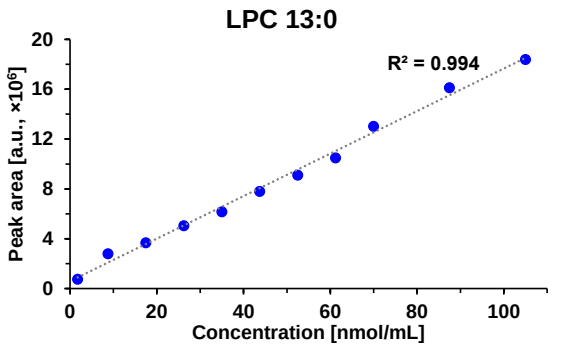
LPC 13:0
R² = 0.994
Peak area [a.u., ×10⁶]
Concentration [nmol/mL]

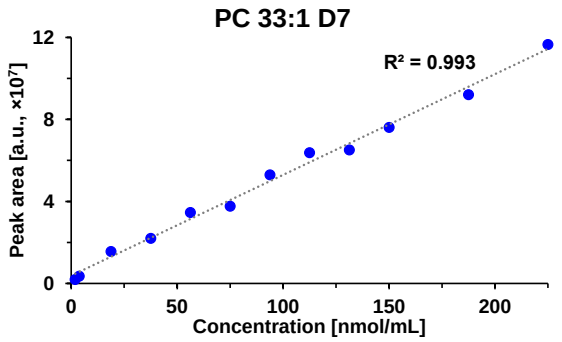
PC 33:1 D7
R² = 0.993
Peak area [a.u., ×10⁷]
Concentration [nmol/mL]

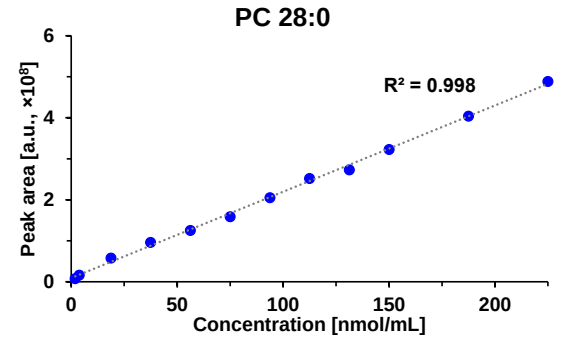
PC 28:0
R² = 0.998
Peak area [a.u., ×10⁸]
Concentration [nmol/mL]

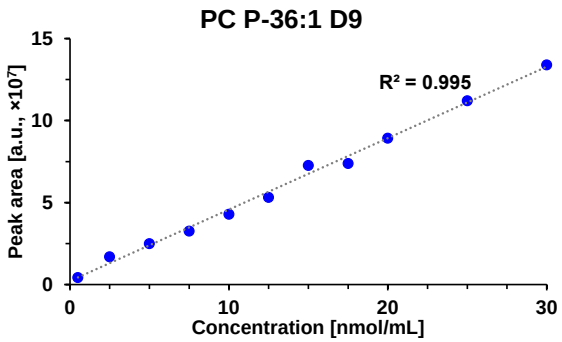
PC P-36:1 D9
R² = 0.995
Peak area [a.u., ×10⁷]
Concentration [nmol/mL]

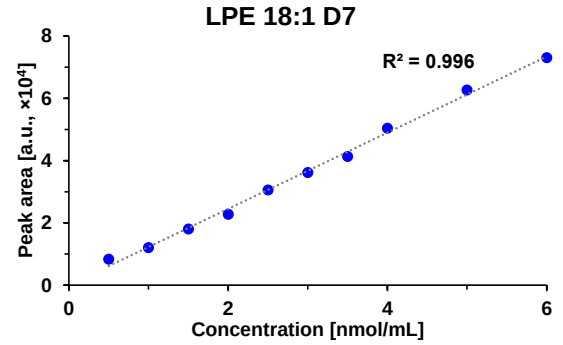
LPE 18:1 D7
R² = 0.996
Peak area [a.u., ×10⁴]
Concentration [nmol/mL]

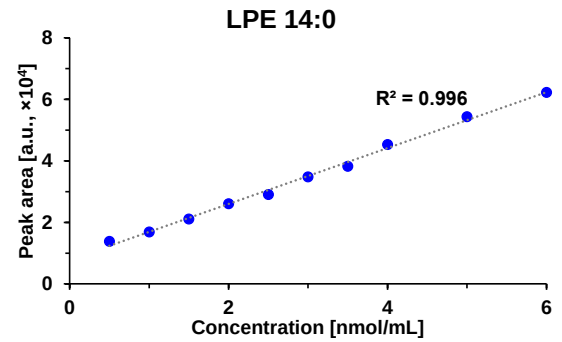
LPE 14:0
R² = 0.996
Peak area [a.u., ×10⁴]
Concentration [nmol/mL]

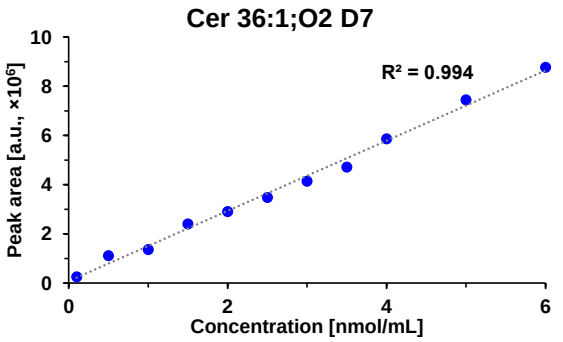
Cer 36:1;O2 D7
R² = 0.994
Peak area [a.u., ×10⁵]
Concentration [nmol/mL]

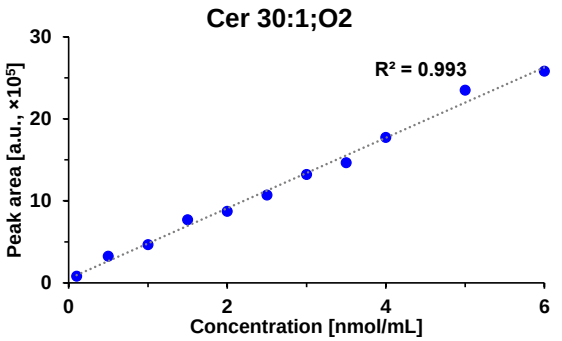
Cer 30:1;O2
R² = 0.993
Peak area [a.u., ×10⁵]
Concentration [nmol/mL]

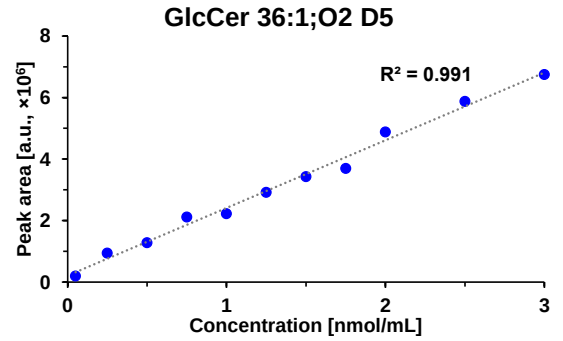
GlcCer 36:1;O2 D5
R² = 0.991
Peak area [a.u., ×10⁶]
Concentration [nmol/mL]

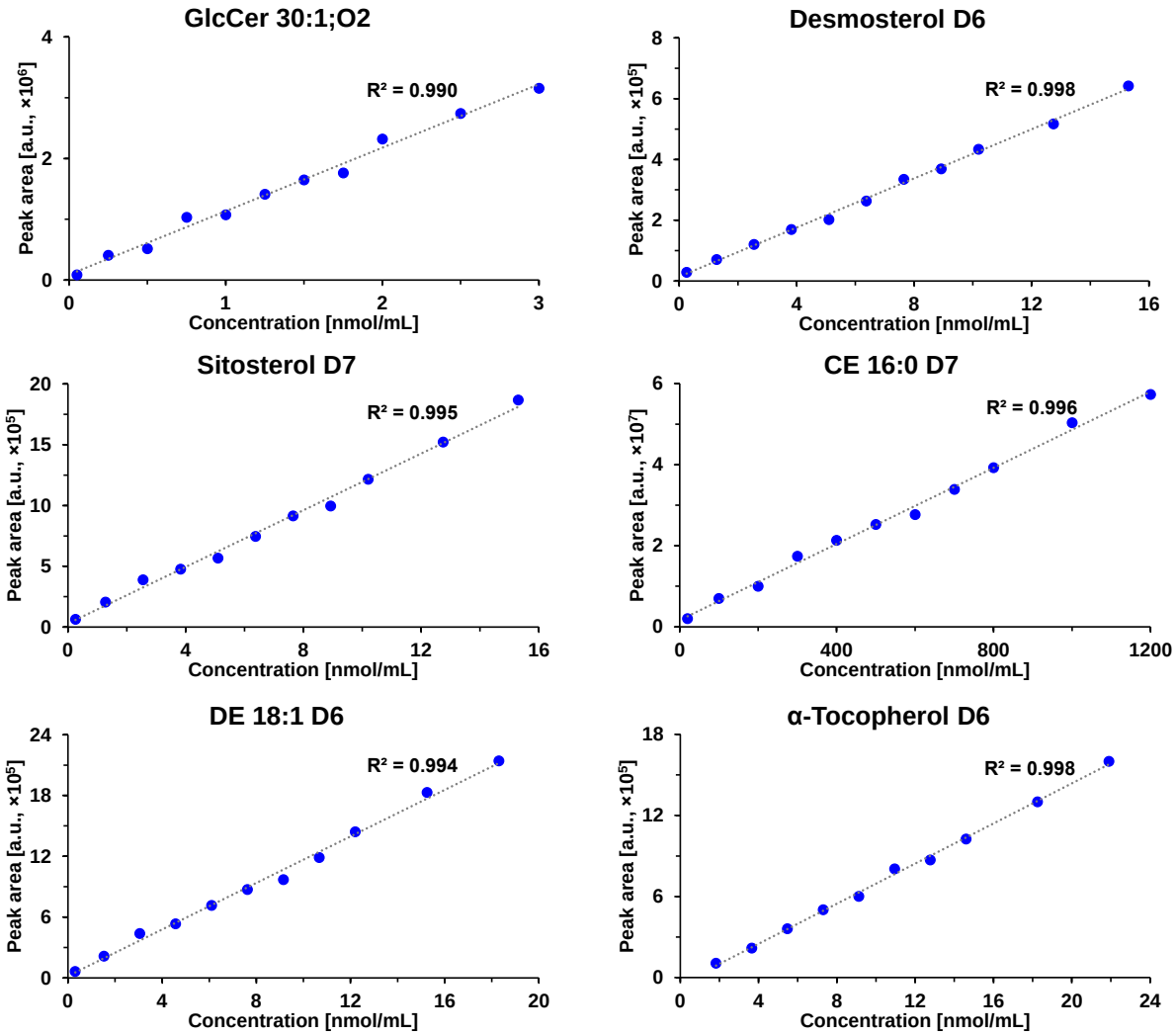


**Figure S3**: Calibration curves of derivatized internal standards in spiked human serum. The data represent the mean values of three independent experiments.

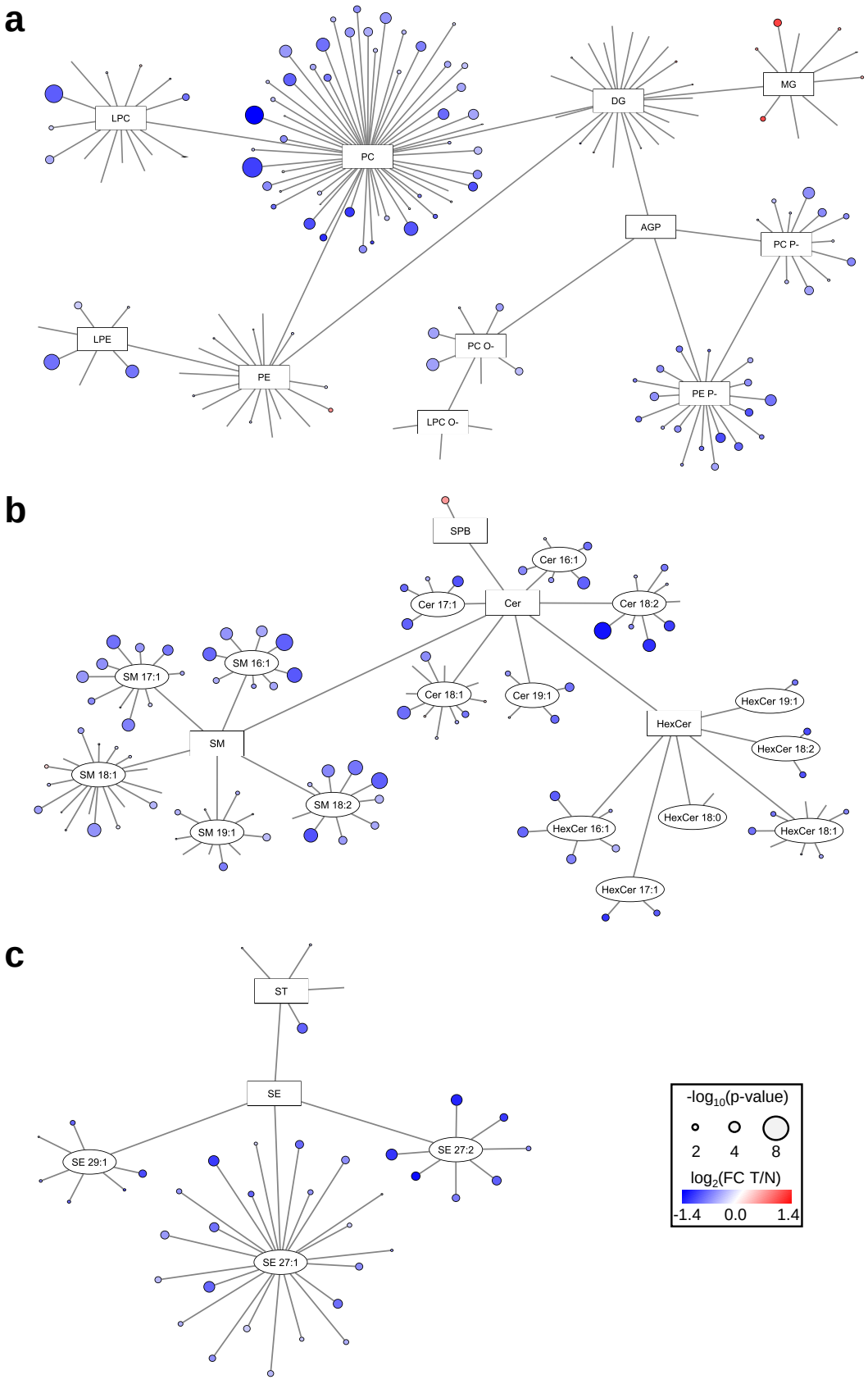


**Figure S4**: Network mapping of lipid species for: **a)** phospholipids and glycerolipids, **b)** sphingolipids, and **c)** sterols, where the size of each circle reflects the *p*-values for individual lipids, and red/blue color saturation represents the fold change (T/N).

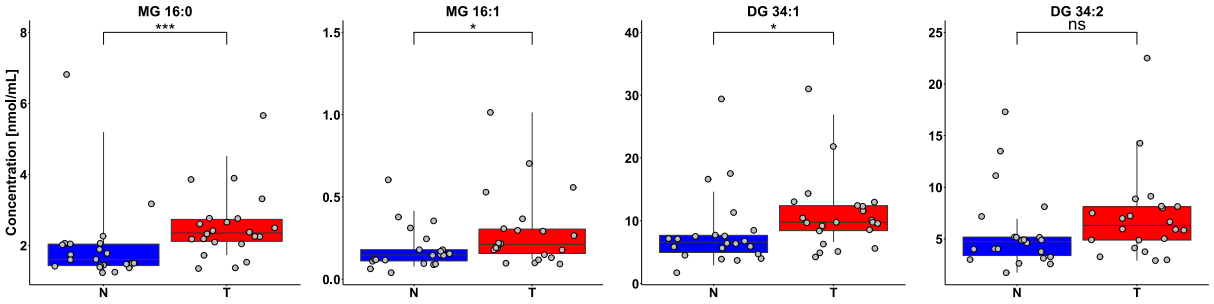


**Figure S5**: Box plots of upregulated glycerolipids showing differences in concentrations between healthy controls (N, blue) and PDAC patients (T, red). The number of significance symbols corresponds to *p*-value ranges from the Mann–Whitney U test, $p > 0.05$ (ns = non-significant), 0.05–0.01 (*), 0.01–0.001 (**), 0.001–0.0001 (***), and <0.0001 (****).

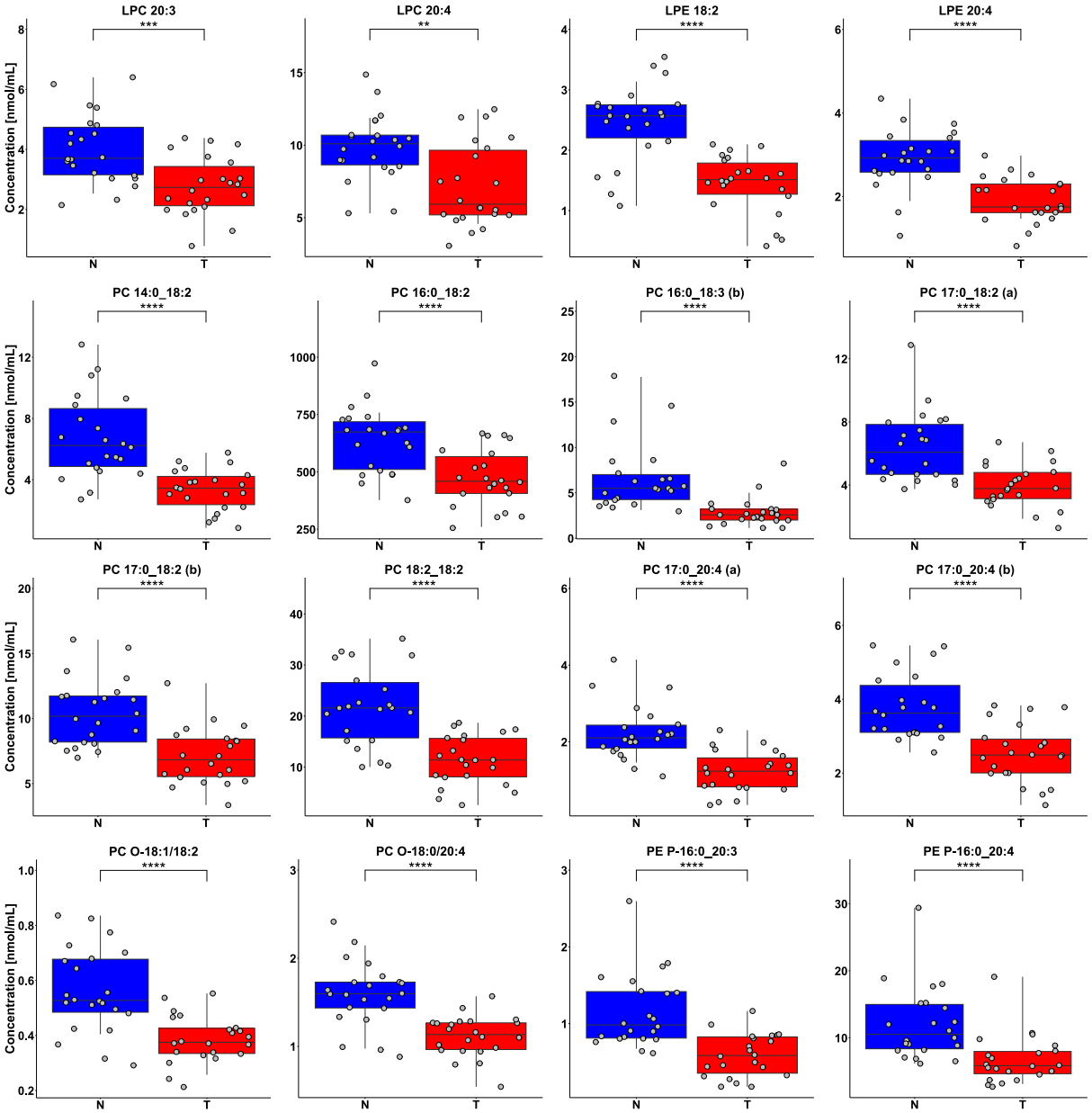


**Figure S6**: Box plots of the most downregulated phospholipids showing differences in concentrations between healthy controls (N, blue) and PDAC patients (T, red). The number of significance symbols corresponds to *p*-value ranges from the Mann–Whitney U test: 0.01–0.001 (**), 0.001–0.0001 (***), and <0.0001 (****).

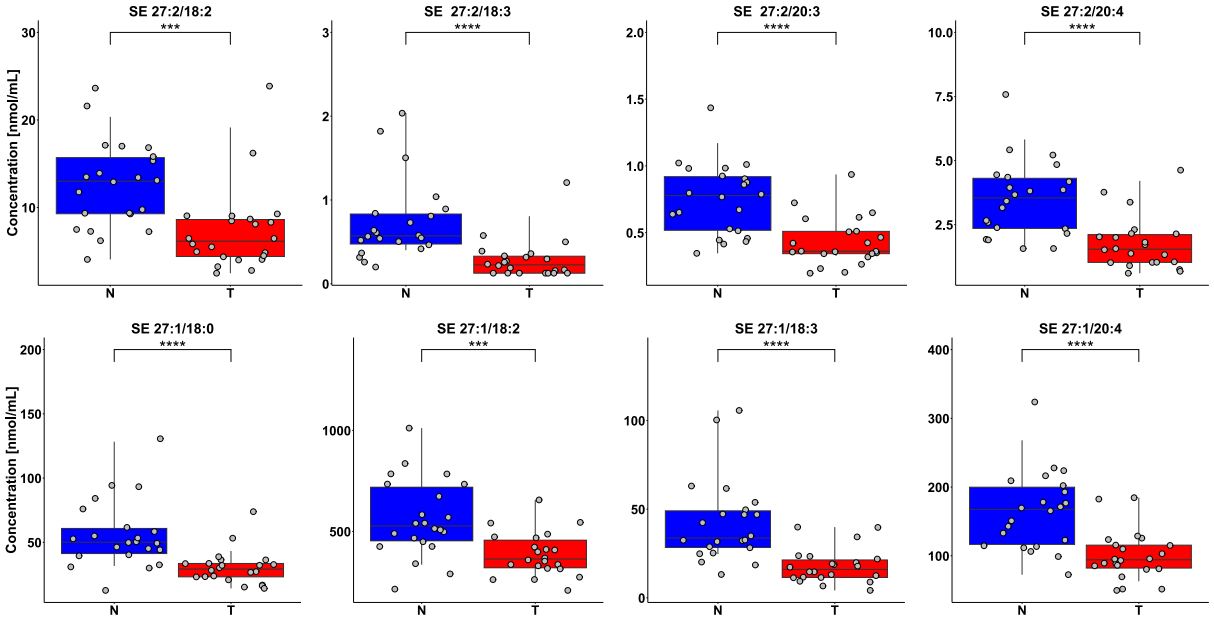


**Figure S7**: Box plots of the most downregulated sterol esters showing differences in concentrations between healthy controls (N, blue) and PDAC patients (T, red). The number of significance symbols corresponds to *p*-value ranges from the Mann–Whitney U test, 0.001–0.0001 (***) and <0.0001 (****).

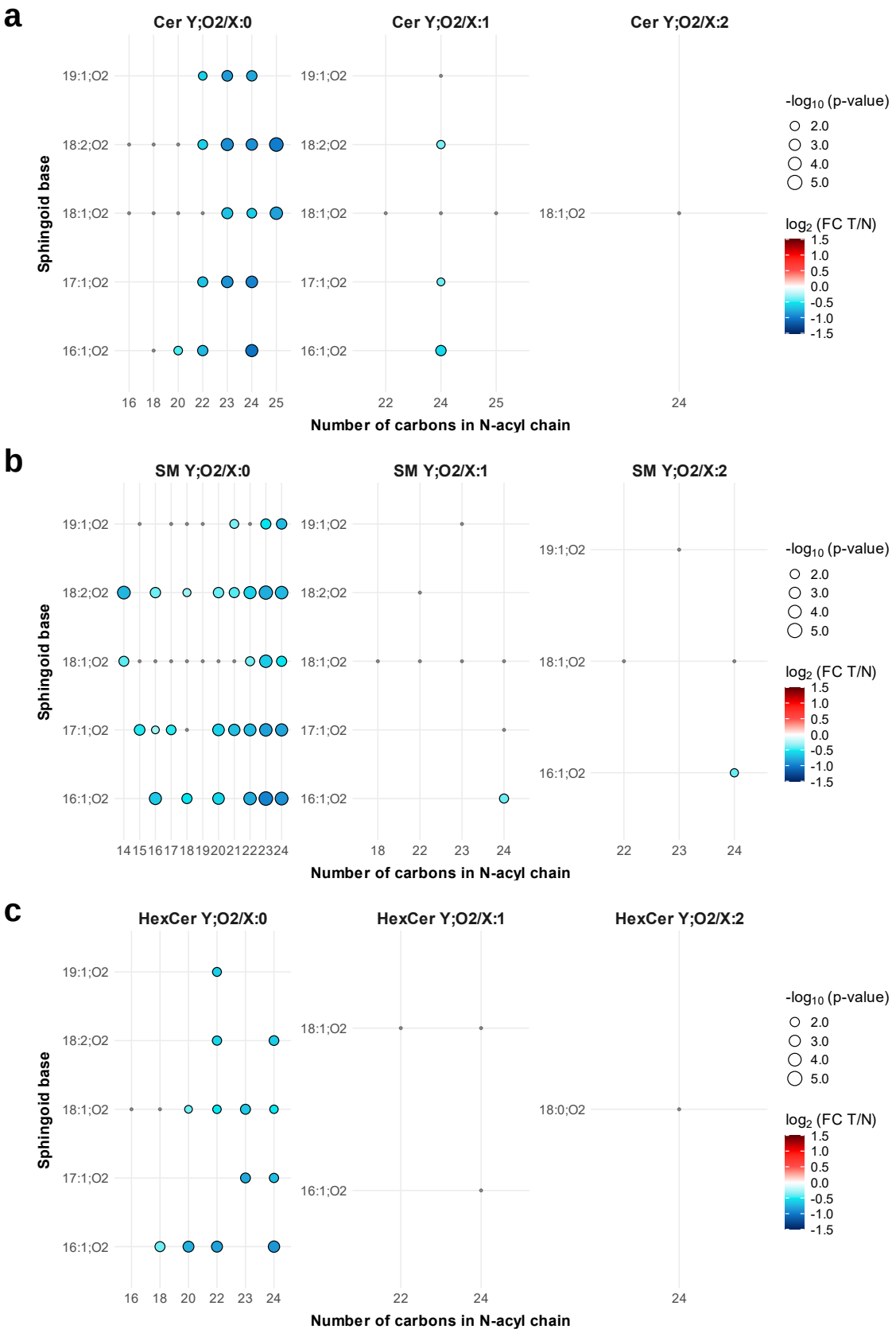


**Figure S8**: Statistical significance for: **a)** ceramides, **b)** sphingomyelins, and **c)** hexosylceramides based on fatty acyl compositions, where Y represents the sphingoid base and X denotes the number of carbons in the *N*-acyl chain.

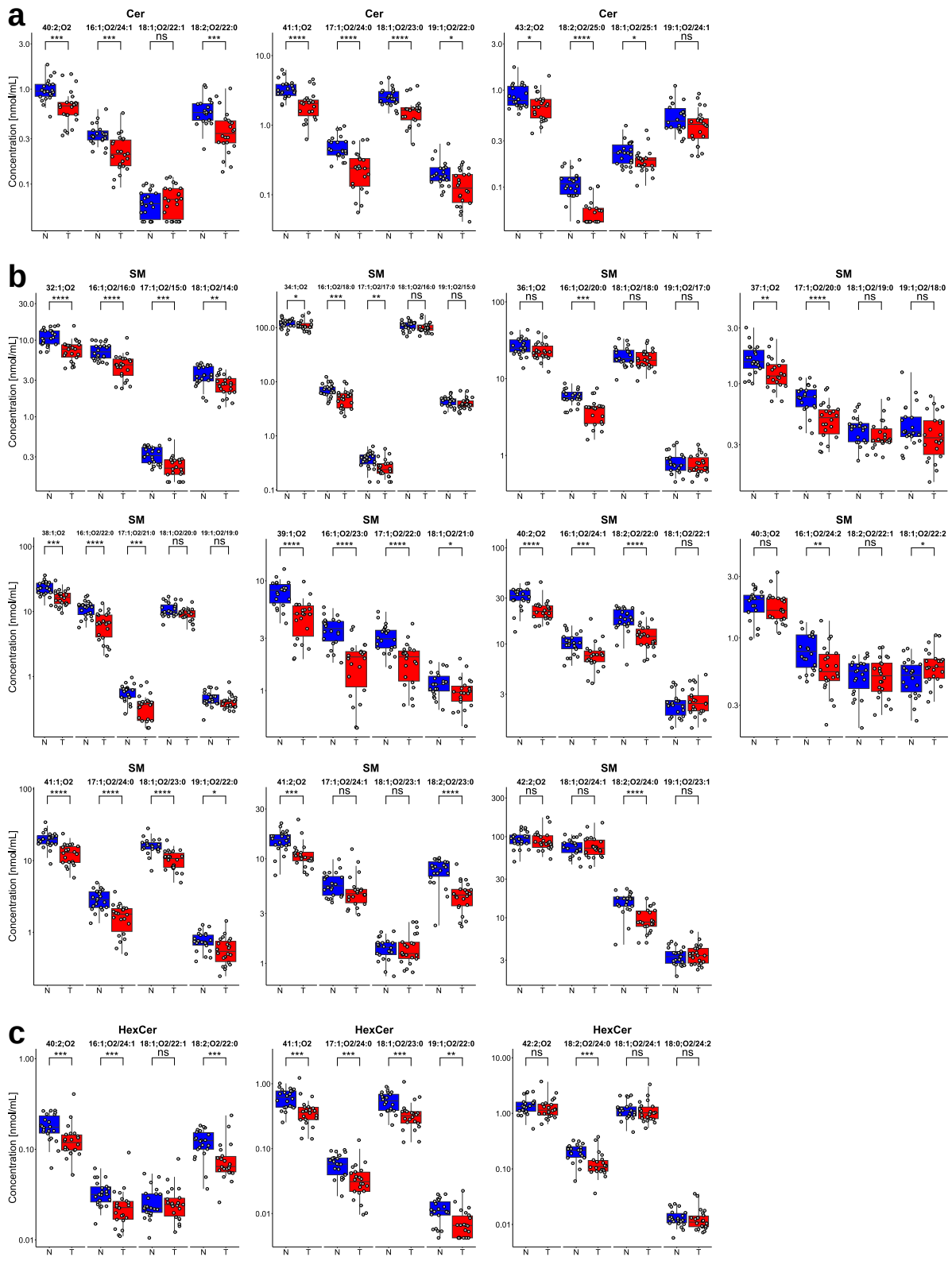


**Figure S9**: Box plots visualizing the effect of fatty acyl composition on the statistical significance of lipid species for: **a)** ceramides, **b)** sphingomyelins, and **c)** hexosylceramides.